JOURNAL OF CATALYSIS 94, 323–334 (1985)

# Discontinuities in the Rate of Sulfur Dioxide Oxidation on Vanadium Catalysts

KE-CHANG XIE[1] AND A. NOBILE, JR.

*College of Engineering, University of South Carolina, Columbia, South Carolina 29208*

Received May 22, 1984; revised February 2, 1985

Through experimental measurements of the intrinsic kinetics of sulfur dioxide ($SO_2$) oxidation on two types of vanadium catalysts and from studies of their thermal and electrical behaviors and the distribution of active components, the reaction rate of $SO_2$ oxidation has been shown to be discontinuous due to a phase transformation of the active components of the catalysts. Accordingly, there appear to be two different temperature ranges in which the reaction takes place: the lower temperature range (LTR) and the higher temperature range (HTR). This phenomenon can be further explained with the idea that the self-poisoning of the catalyst is characterized by a reversible temporality, which comes into effect only at the LTR. © 1985 Academic Press, Inc.

## INTRODUCTION

Catalytic oxidation of sulfur dioxide on vanadium catalysts has been the subject of a wealth of catalytic studies and an important reaction in the industrial production of $H_2SO_4$. A generalization can be made from the more than five dozen intrinsic kinetic equations for vanadium catalysts published up to 1984 (*1–56*) with the following two expressions;

$$r = kf(p_i)(1 - \beta^{1/s}) \quad (1)$$

and

$$r = kf(p_i,T)(1 - \beta^{1/s}), \quad (2)$$

where $r$ is the reaction rate of $SO_2$ oxidation (the conversion rate of $SO_2$), $k$ is the reaction rate constant, $p_i$ is the partial pressure of reaction component $i$, $T$ is the reaction temperature, $f$ is a function based upon the law of mass action and others, $s$ is a stoichiometric number for rate-determining step, if existing, and $\beta$ is defined by

$$\beta = \frac{p_{SO_3}/K_p}{p_{SO_2}p_{O_2}^{1/2}} \quad (3)$$

in which $K_p$ is the equilibrium constant.

[1] Permanent address: Taiyuan University of Technology, Taiyuan, Shanxi, People's Republic of China.

Equations (1) and (2) are commonly used to express reaction rates in heterogeneous catalysis. If $k$ can be described with any accuracy by the Arrhenius equation

$$k = k_0 \exp(-E/RT), \quad (4)$$

where $E$, the activation energy of reactions, is a constant within the reaction temperature range, Eqs. (1) and (2) will be valid in continuous description of the reaction rate of each catalyst examined.

However, there is no commonly accepted rate expression (*5, 8, 9*) consistent with Eqs. (1) or (2) with the capability of describing the $SO_2$ oxidation rate over a wide range of conversions and temperatures. There are two possible reasons for this: first, no ultimate and unambiguous scheme has yet been developed for the mechanism of the chemical reaction on vanadium catalyst (*6*); and second, no agreement has been reached concerning the rate of change of $k$ with temperature. Boreskov *et al.* (*10, 55*) and Kovenklioglu and DeLancey (*9*) found a hysteresis phenomenon in the plane of $k$ versus the reaction temperature and of outlet conversion versus the average feed temperature, respectively. Boreskov *et al.* (*2*), Ivanenko *et al.* (*11*), and Kubota *et al.* (*12*) also reported an



0021-9517/85 $3.00

abrupt change in $E$ in the temperature range 400–470°C. Moreover, some researchers (*1, 5, 13–23*) have noted that a discontinuity exists in the rate of change of $k$ with reaction temperature. Namely, $E$ has two (*5, 9, 13, 14, 16, 17, 21, 22*) or more than two (*19*) differing values in the range of 360–620°C within which the kinetics of the reaction were investigated. But the others (*4, 24–56*), including Mars and Maessen (*24*) and Simecek (*25*)—who had reported, respectively, that $E$ changes from 43 to 19 kcal/mol in the range 397–600°C (*1*) and from 52 to 19 kcal/mol in the range of 460–520°C (*21, 22*)—did not observe any irregular behavior over the same range of temperature.

Therefore, a further test for the discontinuity or the continuity is necessary. The search for a generalized form of the relationship between the reaction rate, the reactant concentration, and the temperature for each catalyst examined should be one of the most important objectives of studies on the kinetics of oxidation of $SO_2$ on vanadium catalysts. Catalyst properties were implicitly contained in the rate constant which reflects the discontinuous or continuous behavior of the rate of $SO_2$ oxidation. Thus, in the study reported here, not only kinetic experiments were carried out, but the physical and chemical properties of the vanadium catalysts were also investigated by means of thermogravimetric and differential thermal analysis, as well as analysis of electric conductivity, X-ray diffraction, and scanning electron microscopy. From these results, we can determine whether or not the kinetic rate discontinuity exists and, if it does, why?

## EXPERIMENTAL

*The reactor system.* The circulation-flow method, which is regarded as a method that affords data corresponding to differential measurement conditions (*6, 57*) is adopted here. The reactor is the internal recirculation type, driven by a pair of magnets

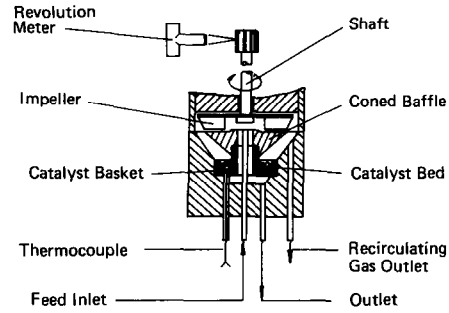


FIG. 1. Reactor and centrifugal impeller.

mounted on the motor shaft and stirring shaft. There is no concentration and temperature gradient in the reaction chamber, so the reactor may be used for measurements of $SO_2$ oxidation rate on the vanadium catalysts in the temperature range of 350–600°C.

The reaction chamber is shown in Fig. 1. Feed gases were prepared by the simultaneous mixing of pure nitrogen, oxygen, and sulfur dioxide gases, then the mixed gases were fed into the reaction chamber at a constant rate (1 atm). The flow rate of nitrogen and oxygen was measured with a mass flow meter and controlled by step-control valves. The flow rate of $SO_2$ was determined by chemical analysis and a thermal conductivity cell. The control of reaction temperature was achieved to 0.5°C/100°C with a temperature-controlling device. The impeller speed (motor revolutions) was determined with a numerical revolution meter.

The effects of interphase and intraparticle transport restrictions have been investigated by changing the flow rate (using different impeller speeds for a constant feed rate) and by variation of the catalyst particle size under well-defined external conditions, respectively. Under the following conditions, the interphase (a) and intraparticle (b) transport restriction should have no effect on the measured conversion rate:

(a) Impeller speed $>$ 3400 rpm (linear velocity of 0.24 m/sec).

(b) Average particle size $\leq$ 0.3 mm.

TABLE 1

Properties of the Vanadium Catalysts Used

| Property | Type A | Type B |
|---|---|---|
| Percentage | | |
| $V_2O_5$ | 7.6 | 6.5 |
| $K_2O$ | 18.3–23.0 | 16.0 |
| $Na_2O$ | 0 | 9.0 |
| Support | Diatomaceous silica | Diatomaceous silica |
| Initial shape | Cylindrical | Cylindrical |
| Initial size (mm) | 5 × 10–15 | 5 × 10–15 |
| Shape of sample Examined | Irregular Particle | Irregular Particle |
| Particle size ($\mu$m) | 370–246 | 370–246 |
| Bulk density of particle (g/ml) | 0.50 | 0.55 |
| Ignition temperature (°C) | 390–400 | 365–375 |

*Catalyst preparation.* Two types of the samples examined, Type A as a $K_2SO_4$–$V_2O_5$ catalyst and Type B as a $K_2SO_4$–$Na_2SO_4$–$V_2O_5$ catalyst, were prepared from corresponding commercial vanadium catalysts provided by Nanjing Chemical Industrial Company, Nanjing, People's Republic of China. The properties of these catalysts are listed in Table 1.

The cylindrical catalysts were first ground to smaller particles in a porcelain mortar. The particles were then sorted using the Tyler Standard screen scale. The samples used were limited to a particle size of ca. 300 $\mu$m. They were divided into six parts for use in kinetic measurement, thermogravimetric, differential thermal, electric conductivity, X-ray diffraction, and scanning electron microscopy analysis. A sample of the catalyst was carefully weighed before measurement and analysis.

*Kinetic studies.* Nine runs of experiments for the reaction rate of $SO_2$ oxidation have been performed on each type of catalyst by changing feed composition and space velocity (SV) under the conditions shown in Table 2. When steady conditions were achieved (ca. 5 h), the conversion of $SO_2$ to $SO_3$ is obtained with the equation

$$x = \frac{a - a_0}{a_0(1 - 0.015a_0)}, \tag{5}$$

where $x$ is the conversion of $SO_2$ to $SO_3$, and $a_0$ and $a$ are the concentration of $SO_2$ in the feed and outlet, respectively. A modified iodimetry chemical analysis was used to measure $SO_2$ in the feed and outlet gases. The reaction rate of $SO_2$ oxidation is calculated from the equation

$$r = 7.44 \times 10^{-7} \frac{a_0 Q_0 x}{\phi W}, \tag{6}$$

where $r$ is the reaction rate of $SO_2$ oxidation, $Q_0$ is the feed flow rate, $W$ is the weight of loaded catalyst sample, and $\phi$ is a volume correction and obtained from

$$\phi = 1 - \frac{a_0 x}{2}. \tag{7}$$

*Thermogravimetric analysis (TGA).* The change in weight of the catalyst samples in a thermogravimetric reactor was determined under different working conditions with a Type TGR-1 thermogravimetric balance. Two parts of the analysis were performed. One is the measurement of the relation between the weight increase and the reaction temperature which was varied stepwise from the low temperature to the high temperature using a temperature controller. Another one in the measurement of the weight increase of catalyst samples ver-

TABLE 2

Reactive Conditions Studied in Kinetic Measurements

| | Type A | Type B |
|---|---|---|
| Sample volume (ml) | 1.6 | 1.6 |
| Reaction temperature (°C) | 380–580 | 370–550 |
| Feed gas composition (%) | | |
| $SO_2$ | 5–15 | |
| $O_2$ | 7–30 | |
| $N_2$ | Remainder | |
| Maximum flow of feed gas at STP (ml/min) | 310 | |
| Impeller speed (rpm) | 3400 | |

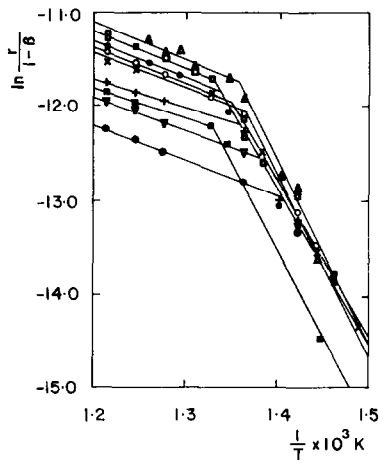


FIG. 2. Dependence of $\ln(r/1 - \beta)$ on $1/T$ for Type A catalyst.

sus the reaction time at certain temperatures.

*Differential thermal analysis (DTA).* The thermal behavior of the vanadium catalysts, Types A and B, for $SO_2$ oxidation has been studied in working state with gas-flow differential thermal analysis (gas-flow DTA). The DTA apparatus permits the same gases to flow simultaneously over reference test particles ($\alpha$-$Al_2O_3$) and working samples. The reaction temperature was varied stepwise using the same temperature controller with that in TGA.

*Electric conductivity analysis (ECA).* The electrical conductivity of the catalyst samples at various temperatures was measured with ECA apparatus consisting of ECA cells containing two electrodes. Electrical conductivity was measured for the samples in air and under reaction condition ($SO_2 + O_2$).

*X-Ray diffraction (XRD) analysis.* The chemical composition change of Types A and B in the $SO_2$ oxidation was qualitatively studied by means of an X-ray diffractometry instrument to acquire more information on the reaction mechanism. A constant scan of 2°/min was used for the $2\theta$ range from 10° to 50°. The X-ray diffraction measurements were performed on the samples of Types A and B which were fresh and used in the kinetic studies of the reaction.

*Scanning electron microscopy (SEM) analysis.* In order to obtain a clear view of the distribution of composition and its change, fresh and used samples were examined with a JEOL JSM-35C electron microscope. The results (Fig. 9) show that the distribution of the active catalyst components has changed.

## RESULTS

### *Kinetic Results*

From Figs. 2 and 3, it can be seen that there is an abrupt change in the reaction rate in the temperature range of 420–480°C for each type of catalyst in all runs. The turning points at which the reaction rate changes sharply with temperature under given conditions are shown in Tables 3 and 4. If the kinetic data could be described by Eq. (1) activation energies could be calculated from Figs. 2 and 3. However, the results of the analysis of the data indicates that Eq. (1) cannot accurately describe the data, since the function $f$ contains temperature (Eq. (2)) (*64*). Therefore, the intrinsic activation energies can not be accurately calculated from Figs. 2 and 3. Nevertheless, an abrupt turn in the activation energies is very clear and definite.

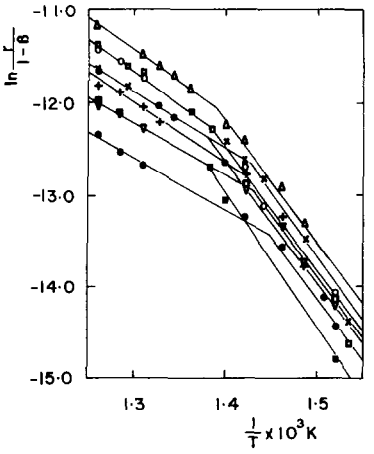


FIG. 3. Dependence of $\ln(r/1 - \beta)$ on $1/T$ for Type B catalyst.

TABLE 3

Turning Points under the Same SV but with Different Feed Composition

| $\frac{p_{SO_2,0}}{p_{O_2,0}}$ | Type A | | Type B | |
|---|---|---|---|---|
| | 6,000[a] | 12,000[a] | 6,000[a] | 12,000[a] |
| 0.37 | 459.4(×) | 462.1(△) | 426.1(×) | 446.2(△) |
| 0.64 | 462.1(+) | 464.8(○) | 431.0(+) | 448.2(○) |
| 0.82 | 473.1(●) | 478.7(□) | 441.1(●) | 461.0(□) |
| 1.00 | 480.0(■) | | 451.4(■) | |

[a] SV ($h^{-1}$).

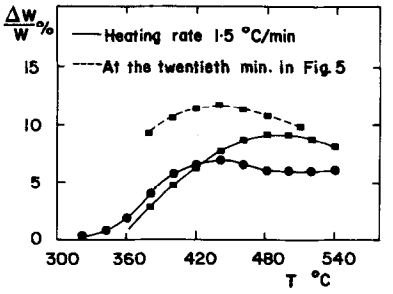


FIG. 4. Relation between weight increase and reaction temperature. Type A (■), and type B (●): Gas composition, 7% $SO_2$, 11% $O_2$, 82% $N_2$; gas flow rate, 100 ml/min; sample size, 0.3 mm; sample weight, 0.3 g.

### *TGA Results*

The experimental results for the TGA are shown in Figs. 4 and 5. From the figures, it can be seen that there is a maximum value of $\Delta W/W$, which can be called weight increase of samples and which is dependent on the reaction time $\tau$ and varies with temperature.

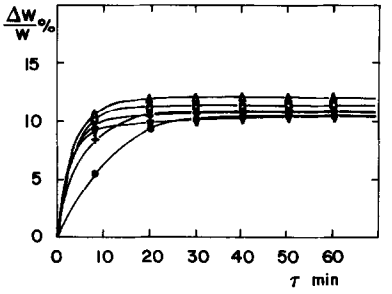


FIG. 5. Weight increase of samples vs reaction time. Sample, Type A. Reaction temperature (°C), (●) 380, (+) 400, (△) 440, (□) 460, (×) 480, (▽) 510. Gas composition, 7% $SO_2$, 19% $O_2$, 74% $N_2$; gas flow rate, 100 ml/min; sample size, 0.3 mm; sample weight, 0.3 g.

### *DTA Results*

From the results (Fig. 6), it can be seen that the exothermic peaks appear clearly at about 445°C in the DTA curve of Type A and about 430°C in the curve of Type B.

### *ECA Results*

From the results (Fig. 7), it can be seen that there is a sharp turn in the curves of both Types A and B.

### *XRD Results*

It has been found that the diffraction pattern and the peak intensities of the used samples are different from those of the fresh ones (Fig. 8).

TABLE 4

Turning Points with the Same Feed Compositions but under Different SV

| SV ($h^{-1}$) | Type A | | | Type B | | |
|---|---|---|---|---|---|---|
| | 0.37[a] | 0.64[a] | 0.82[a] | 0.37[a] | 0.64[a] | 0.82[a] |
| 1,800 | | 436.0(⊖) | | | 416.5(⊖) | |
| 3,600 | | 448.3(▽) | | | 423.7(▽) | |
| 6,000 | 459.4(×) | 462.1(+) | 473.1(●) | 426.1(×) | 431.0(+) | 441.1(●) |
| 12,000 | 462.1(△) | 464.8(○) | 478.7(□) | 446.2(△) | 448.2(○) | 461.0(□) |

[a] $p_{SO_2,0}/p_{O_2,0}$.

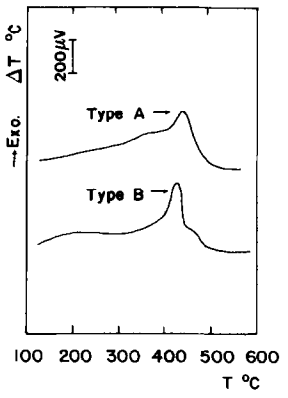


FIG. 6. DTA curves of samples. Gas composition, 7% $SO_2$, 11% $O_2$, 82% $N_2$; gas flow rate, 100 ml/min; heating rate, 4.5°C/min; sample size, 0.3 mm; reference particle size, 0.3 mm.

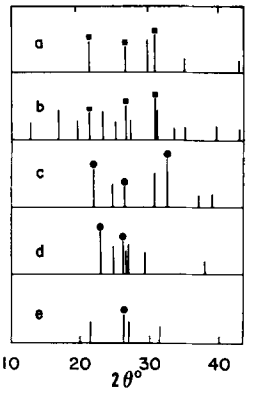


FIG. 8. X-Ray diffraction patterns of fresh and used samples. (a) Fresh sample of Type A, (b) Type A used for 6 h at 470°C in reaction atmosphere, (c) fresh sample of Type B, (d) Type B used for 10 h at 438°C in reaction atmosphere, (e) Type B used for 20 h at 480°C in reaction atmosphere.

### *SEM Results*

The results (Fig. 9) show that the distribution of the active catalyst components has changed after exposure to reaction conditions.

All the experimental results indicate that the physical and chemical properties of the $K_2SO_4$–$V_2O_5$ and $K_2SO_4$–$Na_2SO_4$–$V_2O_5$ catalysts under reaction conditions changed in the temperature range of 430–480°C. There is a corresponding specific temperature range for each change (Table 5).

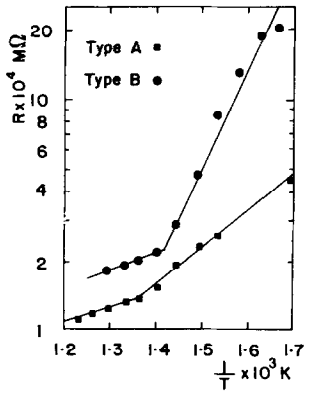


FIG. 7. ECA curves of samples. Type A, after being saturated for 2 h in an atmosphere with 5% $SO_2$; Gas composition, 7% $SO_2$, 11% $O_2$, 82% $N_2$. Type B, after saturated for 1 h in an atmosphere with 1% $SO_2$; Gas composition, air.

## DISCUSSION

The change in physical and chemical properties is due to a phase transformation of the active components of the catalyst, $K_2SO_4$–$V_2O_5$ or $K_2SO_4$–$Na_2SO_4$–$V_2O_5$, for the following reasons:

(1) The experimental value of $\Delta W/W$ after chemisorption of $SO_2$ by the samples in the melt phase is approximately the same as the $\Delta W/W$ when calculated according to the

TABLE 5

Change of Catalyst Behaviors and the Temperature for Them to Occur

| Experimental | Change observed | Occurring temperature (°C) | | Fig. |
|---|---|---|---|---|
| | | Type A | Type B | |
| TGA | Maximum $\Delta W/W$ | 440<br>480[a] | 440[a] | 4 |
| DTA | Exothermal peak | 445 | 430 | 6 |
| ECA | Abrupt change | 462 | 431 | 7 |
| XRD | Change of intensity and distribution of characteristic lines | | 438 | 8 |
| SEM | Change of distribution of active components | | 438 | 9 |

[a] The changing rate of $\Delta W/W$ may be smaller than the heating rate of catalyst samples.

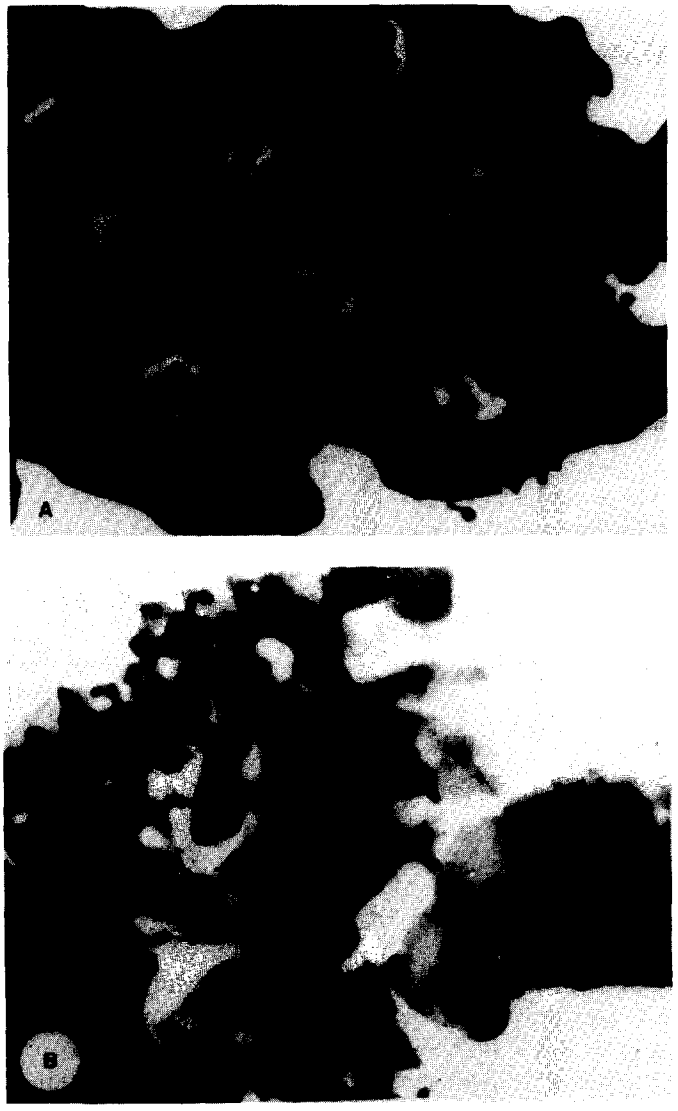


FIG. 9. (A) SEM microphotograph of fresh sample, the same sample as c in Fig. 8. (B) SEM microphotograph of used sample, the same sample as d in Fig. 8.

following chemical equations:

$$V_2O_5 + SO_2 \leftrightarrows V_2O_5 \cdot SO_2(\rightarrow V_2O_4 \cdot SO_3) \quad (8)$$

and

$$K_2SO_4 + SO_2 \leftrightarrows K_2S_2O_7. \quad (9)$$

Assuming that Eqs. (8) and (9) take place, the weight increase of the sample, $\Delta W$ (the amount of $SO_2$ absorbed), can be calculated from the amount of the active component present in the sample. For example, with reference to Type A, $\Delta W/W$ was calculated to be 0.121 g/g, which is greater than the $\Delta W/W$ values obtained experimentally in the lower temperature range (LTR), as seen in Fig. 4. This indicates absorption of $SO_2$ in the liquid phase in the HTR. The $\Delta W/W$ values in Fig. 4 increase with temperature. The maximum value of $\Delta W/W$ occurs at approximately the temperature at which the active components are transformed from a

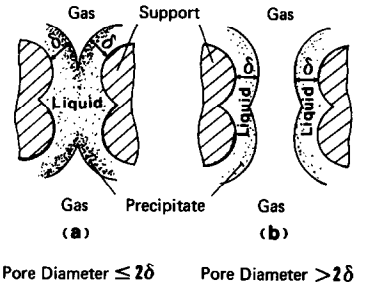


FIG. 10. Liquid distribution on the support and self-poisoning.

solid phase to solid–liquid. When the reaction temperature is increased further, $\Delta W/W$ decreases due to desorption of $SO_3$.

(2) Figure 7 shows how the electrical resistivity increases more rapidly below the temperatures of 462 and 431°C for catalysts of Types A and B, respectively. This may be due to decreased ionic conduction in the solid phase.

(3) the X-ray diffraction patterns in Fig. 8 show that the distribution of active components has changed and some intermediates are formed. The SEM photomicrographs of fresh and unused catalyst samples indicate that some spreading of the surface components has occurred during the reaction. Figure 9A shows the active components to appear as uniform droplets on the support surface. Figure 9B suggests that the support surface has become wet with the active components due to phase transformation during reaction.

From the fact that the equilibrium $\Delta W/W$ values are close at various reaction temperatures (Fig. 5) and that there is no appearance of an obvious endothermic peak (Fig. 6) in the phase transformation, it can be supposed that the phase transformation does not occur abruptly. If the phase transformation occurred abruptly, high values of $\Delta W/W$ would be seen for higher temperatures and lower values seen at the lower temperatures. Figure 5 shows the values to be somewhat closer together, indicating slower transformation. As the active components become more molten, the $SO_2$ oxidation would go on, and the reaction heat released would be greater than the heat absorbed by the phase transformation. This accompanying process will stop as soon as the phase transformation is completed. Thus the reaction rate becomes greater. Accordingly, a sharp exothermic peak is observed.

The phase transformation of the active components of the catalysts is the main reason for the discontinuities in the rate of $SO_2$ oxidation, and the transformation apparently results in the temporal self-poisoning of the vanadium catalysts in the lower temperature range (LTR). The temporal self-poisoning, as it is called, is reversible, as explained in the following. The vanadium catalyst is transformed into a supported liquid phase (SLP) catalyst under the working conditions (*58–61*). If $\delta$ is defined as the thickness of the liquid phase, the liquid distribution on the support may be classified into two categories, depending upon the pore size of the support (Fig. 10). Despite the larger pores (pore diameter $> 2\delta$), the active components exist in a SLP state which is of higher viscosity in the LTR. Thus, a uniform liquid distribution (i.e., no agglomeration of the liquid) might not appear in the pores of the support. As a result, the solid–liquid would agglomerate at the mouth of the pores and cause blocking of the pores. The chemisorption of $SO_2$, step 1 of the catalytic oxidation of $SO_2$, by the active components would thus be difficult. Even though the chemisorption took place, self-poisoning of the catalysts would result from the lower solubility and lower activity of the reduced intermediate vanadium compound. The self-poisoning causes a decrease in the available surface area when the active components are molten (Fig. 10a), and a selective poisoning (i.e., the poisoning of pore mouth) occurs when larger pores are not blocked off (Fig. 10b). Consequently, the reoxidation of the reduced intermediate vanadium compound, step 2 of the catalytic oxidation of $SO_2$, will also be difficult, and the resulting precipita-

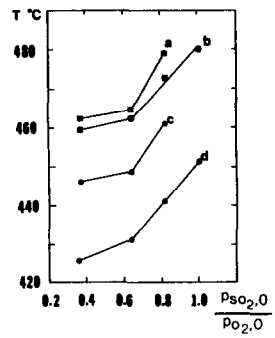


FIG. 11. Relation between turning temperatures and $p_{SO_2,0}/p_{O_2,0}$ ratio in the feed gases

| Curve | Type | SV ($h^{-1}$) |
|---|---|---|
| a | A | 12,000 |
| b | A | 6,000 |
| c | B | 12,000 |
| d | B | 6,000 |

tion of a $V^{4+}$ compound may gradually deplete the liquid phase of active vanadium species.

The effect of the blocking of the pores and the precipitation of the $V^{4+}$ form of the catalyst is to cause higher values for the activation energy in the LTR. However, the poisoning is not permanent and can be recovered by raising the temperature. The activity of the catalyst will increase with the raising of reaction temperature or oxygen content of the gas mixture. Under the same SV, increasing $O_2$ content of the feed gases (i.e., decreasing the ratio of $p_{SO_2,0}/p_{O_2,0}$) will increase the degree of conversion of $SO_2$; i.e., $p_{SO_3}/p_{SO_2}$ ($= x/1 - x$) will be greater. Because the $p_{SO_3}/p_{SO_2}$ ratio is in equilibrium with $V_2O_4 \cdot SO_3/V_2O_5 \cdot SO_2$ in the active melt (*1*), the latter will increase as well. Therefore, it becomes easier for step 2 to occur, and the activity of the catalyst will be recovered in the LTR. This situation is the reason why the turning temperature is lower under the condition of lower $p_{SO_2,0}/p_{O_2,0}$ ratio and of the same SV (Fig. 11). In addition, if the $p_{SO_2,0}/p_{O_2,0}$ ratio is a constant, the degree of conversion will increase, and the turning temperature decreases with decreasing SV (Fig. 12).

As already mentioned, the turning temperature as a function of the degree of conversion (Fig. 13) and its change may be caused by the change of the valence number and of the composition of vanadium species. In the HTR, the active components are molten and the available surface area is larger. The reaction occurs not only on the surface of the catalysts but also in the melt (*61*). Thus, the activity of the vanadium catalysts is greater and activation energy of the reaction is lower. There is an

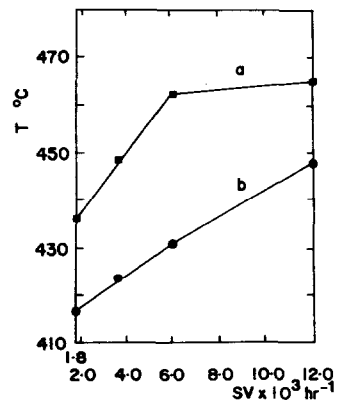


FIG. 12. Relation between turning temperatures and SV $p_{SO_2,0}/p_{O_2,0} = 0.64$. (a) Type A and (b) Type B.

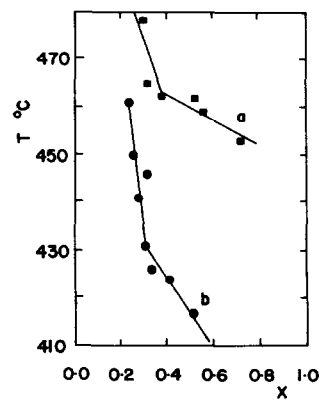


FIG. 13. Relation between turning temperatures and conversion $x$. (a) Type A and Type B.

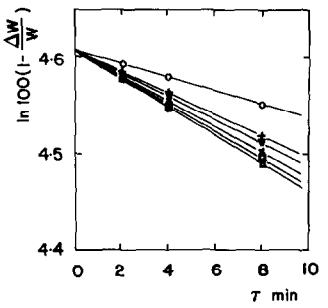


FIG. 14. A pseudo-first-order reaction, plotted according to Eq. (10).

optimum value at which the catalysts show a maximum activity (*61, 62*). Since the optimum value depends mostly on the $O_2$ content of the gas mixture, SV, degree of conversion, etc., it is likely that there exist corresponding breakpoints on the curves of the turning temperature versus these various factors (Figs. 11–13).

It is of interest that the break of the rate constant ($k''$) of pseudo-first-order thermogravimetric reaction on the Arrhenius plot also displays the discontinuities in the rate of $SO_2$ oxidation. The thermogravimetric reaction is pseudo-first order (Fig. 14) at its earlier stage (Fig. 5) because it can be described more accurately by the first-order rate equation

$$\frac{d(\Delta W/W)}{d\tau} = k''(1 - \Delta W/W). \qquad (10)$$

Separating the variables and integrating results in the equation

$$\ln(1 - \Delta W/W) = k''\tau. \qquad (11)$$

As shown in Fig. 15, the curve of ln $k''$ versus $1/T$ shows two different slopes which go in opposite directions at ~440°C. From this fact, it might be considered that the enthalpy change of the thermogravimetric reaction has a positive value at the LTR but is negative at higher values.

There are two explanations for the differences between the behaviors of samples Types A and B in the reaction.

First, the chemisorption and diffusion of oxygen by the molten active components are greater in the presence of $Na^+$ in Type B, and the reoxidation of the reduced intermediate vanadium compound is easier. The (K + Na)/V ratio (= 4.5) of Type B is greater than the K/V ratio (= 2.7) of Type A, so more $M_2S_2O_7$ ($M$ = K,Na) can be formed in Type B under the reaction conditions. As a result, the solubility of the reduced intermediate vanadium compounds may be increased, and their precipitation from the liquid phase may be prevented. Therefore, the activity of Type B is greater than that of Type A, and its activation energy is less than Type A in the LTR.

Second, the presence of $Na^+$ in sample B might disturb the uniformity of the negative ions surrounding the $V^{4+}$ species and promote the reoxidation of the $V^{4+}$ species under the reaction conditions. This process could probably be influenced by the $p_{SO_3}/p_{SO_2}$ ratio, so that a small change of the degree of conversion of $SO_2$ would, as shown in Fig. 13, bring about a notable change of the turning temperature of Type B, especially in the LTR.

## SUMMARY

The experimental results furnish many arguments in favor of the existence of the reaction rate discontinuity of $SO_2$ oxidation on the vanadium catalysts in the whole reaction temperature range, but the rate is

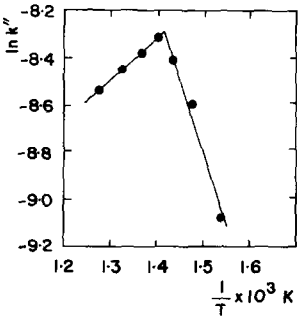


FIG. 15. Temperature dependence of the rate constant $k''$ for the pseudo-first-order thermogravimetric reaction.

TABLE 6

Parameter Values of the Rate Discontinuities Equation

| Parameter | Type A | | Type B | |
|---|---|---|---|---|
| | 380–470°C | 470–580°C | 370–440°C | 440–550°C |
| $k_0$ | $3.035 \times 10^7$ | 15.63 | $9.310 \times 10^5$ | 18.12 |
| $E$ (cal/mol) | 40,394.5 | 18,861 | 35,508 | 18,664.9 |
| $K_2$ | $1.943 \times 10^{-7}$ | $1.111 \times 10^{-5}$ | 0 | $1.839 \times 10^{-5}$ |
| $Q_2$ (cal/mol) | 17231.8 | 13316 | — | 13,285.5 |
| $K_3$ | $3.021 \times 10^4$ | $5.019 \times 10^4$ | 0 | $2.889 \times 10^4$ |
| $Q_3$ (cal/mol) | −16,519.8 | −16,484.2 | — | −16,436.8 |
| $l$ | 0.65 | 0.55 | 0.50 | 0.63 |

continuous in the LTR and HTR, respectively. The change of the turning point is a function of the degree of $SO_2$ conversion under the reaction conditions. The discontinuities of the reaction rate are primarily caused by the phase transformation of active components in the catalysts, and the phase state is gradually transformed. The precipitation of the reduced intermediate vanadium compound that may deplete the molten phase of active vanadium species leads to the peculiar and temporal self-poisoning of the catalysts. Consequently, the activation energy of $SO_2$ oxidation is not a constant in the whole reaction temperature range but is greater in LTR than in HTR. From the results of a study of intrinsic kinetics for $SO_2$ oxidation on the vanadium catalysts, it may be shown that the rate discontinuities could be described by the same mathematical model:

$$r = \frac{k_0 \exp(-E/RT) p_{SO_2} p_{O_2}^{l} (1 - \beta)}{p_{SO_2} + K_{2,0} \exp(Q_2/RT) p_{O_2}^{l} + K_{3,0} \exp(Q_3/RT) p_{SO_3}} \quad (12)$$

with the corresponding characteristic parameter values as shown in Table 6 (*63, 64*).

ACKNOWLEDGMENTS

We are greatly indebted to Professors H. X. Guo, Z. H. Han, and F. F. Huang, for their valuable advice. We would like to express sincere thanks to Dr. J. G. McCarty, who offered many suggestions which proved to be very helpful in the completion of this paper.

REFERENCES

1. Mars, P., and Maessen, J. G., "Proceedings, 3rd International Congress on Catalysis, Amsterdam, 1964," Vol. 1, p. 266. Wiley, New York, 1965.
2. Boreskov, G. K., Buyanov, R. A., and Ivanov, A. A., *Kinet. Katal.* **8,** 153 (1967).
3. Weychert, S., and Urbanek, A., *Int. Chem. Eng.* **9,** 396 (1969).
4. Harris, J. L., and Norman, J. R., *Ind. Eng. Chem. Process Des. Dev.* **11,** 564 (1972).
5. Livbjerg, H., and Villadsen, J., *Chem. Eng. Sci.* **27,** 21 (1972).
6. Urbanek, A., and Trela, M., *Catal. Rev.-Sci. Eng.* **21,** 73 (1980).
7. Xie, K. C., *Taiyuan Gongxueyuan Xuebao* **26,** 101 (1981); *Chem. Abstr.* **96,** 58463b.
8. Weychert, S., and Urbanek, A., *Przem. Chem.* **47,** 727 (1968).
9. Kovenklioglu, S., and DeLancey, G. B., *Canad. J. Chem. Eng.* **57,** 165 (1979).
10. Boreskov, G. K., *"Kataliz v Proizvodstve Sernoi Kisloty."* Goskhimizdat, Moscow, 1954.
11. Ivanenko, S. V., Torocheshnikov, N. S., and Saltanova, V. P., *Khim. Promst.* **48,** 847 (1972).
12. Kubota, M., Ishizawa, M., and Shindo, M., *Ryusan* **12,** 243 (1959).
13. Calderbank, P. H., *J. Appl. Chem.* **2,** 482 (1952).
14. Calderbank, P. H., *Chem. Eng. Prog.* **49,** 585 (1953).
15. Eklund, R. B. "The Rate of Oxidation of Sulfur Dioxide with a Commercial Vanadium Catalyst." Almquist-Wiksell, Stockholm, 1956.
16. Zhang, M. Z., Guo, S. D., Wang, S. J., Weng, W. S., and Chen, Y., *Huagong Xuebao* **2,** 137 (1957).
17. Rszyev, P. B., Royter, U. A., and Korneychuk, G. P., *Ukr. Khim. Zh.* **26,** 161 (1960).

18. Ishii, T., *Kagaku Kogaku* **4,** 122 (1966).
19. Ivanov, A. A., and Boreskov, G. K., *Kinet. Katal.* **9,** 560 (1968).
20. Michalek, J., and Vosolsobe, J., *Chem. Prum.* **17,** 527 (1967).
21. Simecek, A., Michalek, J., and Regner, A., *Collect. Czech. Chem. Commun.* **33,** 2709 (1968).
22. Simecek, A., Regner, A., and Vosolsobe, J., *Collect. Czech. Chem. Commun.* **33,** 2162 (1968).
23. Mukhlenov, I. P., Malkiman, V. I., and Kravchenko, E. A., *Zh. Prikl. Khim. (Leningrad)* **42,** 1823 (1969).
24. Mars, P., and Maessen, J. G., *J. Catal.* **10,** 1 (1968).
25. Simecek, A., *J. Catal.* **18,** 83 (1970).
26. Matsui, M., and Kiyoura, R., *J. Soc. Chem. Ind. Jpn.* **40,** 465 (1937).
27. Boreskov, G. K., and Sokolova, F. I., *Zh. Prikl. Khim.* **14,** 1240 (1937).
28. Krichevskaya, E. L., *Zh. Fiz. Khim.* **21,** 187 (1947).
29. Colette, F., and Scheepers, L., *Chim. Ind.* **63,** 246 (1950).
30. Baron, T., Manning, W. R., and Johnstone, H. F., *Chem. Eng. Prog.* **48,** 125 (1952).
31. Mars, P., and van Krevelen, D. W., *Chem. Eng. Sci.* **3,** 41 (1954).
32. Goldman, M., Canjar, L. N., and Beckman, R. B., *J. Appl. Chem.* **7,** 274 (1957).
33. Zakarevski, M. S., and Zhang, M. Z., *Acta Sci. Nat.* **1,** 117 (1958).
34. Hara, H., *Ryusan* **8,** 161 (1955).
35. Hara, H., *Ryusan* **11,** 186, 228, 267 (1958).
36. Hara, H., *Ryusan* **12,** 155, 209 (1959).
37. Hara, H., Adachi, A., and Kurata, N., *Kogyo Kagaku Zasshi* **62,** 669 (1959).
38. Hara, H., Adachi, A., and Kurata, N., *Kogyo Kagaku Zasshi* **63,** 56 (1960).
39. Schytil, F., and Schwalb, H., *Chem. Eng. Sci.* **14,** 367 (1961).
40. Davidson, B., and Thodos, G., *AIChE J.* **10,** 568 (1964).
41. Mathur, G. P., and Thodos, G., *Chem. Eng. Sci.* **21,** 1191 (1966).
42. Brusset, H., and Luquet, F., *Genie Chem.* **96,** 557 (1966).
43. Regner, A., and Simecek, A., *Collect. Czech. Chem. Commun.* **33,** 2540 (1968).
44. Zinger, G. I., and Vasil'eva, L. P., "Sbornik Promyshlennosti Udobrenii i Sernoi Kisloty," NIUIF. M. vyp. 3, 5 1967.
45. Hullet, J. R., and Wilson, W., *J. Chem. Soc. A.* **10,** 2569 (1968).
46. Glueck, A. R., and Kenney, C. N., *Chem. Eng. Sci.* **23,** 1257 (1968).
47. Collina, A., Corbetta, A., and Capelli, A., *in* "European Symposium on the Use of Computers in the Studies Preceding the Design of Chemical Plants, 97th Event of European Federation of Chemical Engineering." Paper No. 2-8, Firenze, 1970.
48. Pomerantsev, V. M., *Zh. Prikl. Khim.* **43,** 423 (1970).
49. Traina, F., Curchetto, M., Capelli, A., Colina, A., and Dente, M., *Chim. Ind. (Milan)* **52,** 329 (1970).
50. Neth, N., Kautz, G., Huster, H. J., and Wagner, V., *Chem. Ing. Tech.* **51,** 825 (1979).
51. Kokhreidze, R. K., Ivanenko, S. V., Saltanova, V. P., and Torocheshnikov, N. S., *Khim. Promst.* **(9),** 556 (1979).
52. Slavin, G. Ts., Soroko, V. E., and Prokopenko, A. N., *Zh. Prikl. Khim.* **53,** 2187 (1980).
53. Ponomarev, V. E., and Geier, S. E., Deposited Doc. VINITI 5163-81, 85 (1981).
54. Szarawar, J., Kozik, C., and Aniol, S., *Przem. Chem.* **61,** 454 (1982).
55. Bal'zhinimaev, B. S., Kozyrev, S. V., Boreskov, G. K., Ivanov, A. A., Belyaeva, N. P., and Zaikovskii, V. I., *Geterog. Katal., Mater. Vses. Konf. Mekh. Katal. Reakt. 3rd,* 177 (1982).
56. Lu, C. Q., Peng, Y. H., Chen, Q. X., and Zhang, C. L., *Huagong Xuebao* **1,** 58 (1983).
57. Livbjerg, H., and Villadsen, J., *Chem. Eng. Sci.* **26,** 1495 (1971).
58. Villadsen, J., and Livbjerg, H., *Catal. Rev.-Sci. Eng.* **17,** 203 (1978).
59. Boreskov, G. K., Dzis'ko, V. A., Tarasova, D. V., and Balaganskaya, G. P., *Kinet. Katal.* **11,** 181 (1971).
60. Gavrilov, V. Yu., Fenelonov, V. B., Samakhov, A. A., Ivanov, A. A., and Boreskov, G. K., *Kinet. Katal.* **19,** 428 (1978).
61. Xie, K. C., *Taiyuan Gongxueyuan Xuebao* **30,** 108 (1982); *Chem. Abstr.* **98,** 167700p.
62. Xie, K. C., *Taiyuan Gongxueyuan Xuebao* **31,** 94 (1982); *Chem. Abstr.* **101,** 98444z.
63. Guo, H. X., Han, Z. H., and Xie, K. C., *Huagong Xuebao* **2,** 139 (1984); *Chem. Abstr.* **101,** 98434w.
64. Guo, H. X., Han, Z. H., and Xie, K. C., *Huagong Xuebao* **3,** 244 (1984); *Chem. Abstr.* **102,** 51555s.